Thiam, A., Martinez-Cisneros, C., Molméret, Y., Iojoiu, C. & Sanchez, J. Y. (2019). PEO: An immobile solvent? *Electrochimica Acta*, vol. 302, pp. 338–343.

DOI: 10.1016/j.electacta.2019.02.005

PEO: an Immobile Solvent?

A.Thiam[1], C.Martinez-Cisneros[2], Y.Molméret[1], C.Iojoiu[1], J-Y.Sanchez[1,2]

[1] Univ. Grenoble Alpes, CNRS, Grenoble INP, LEPMI, 38000 Grenoble, France.

[2] Materials Science and Engineering Department, University Carlos III of Madrid, Spain.

Abstract

Despite used for half a century as host for salt-polymer complexes, PEO is still not a fossil and due to its availability, remains regularly used as a reference in solvent-free polymer electrolytes and related electrochemical cells. Often qualified as macromolecular solvent or immobile solvent, its drawbacks (crystallinity, mechanical strength) are well identified. On the other hand, its electrolyte conductivity maxima are considered as the best possible in absence of molecular solvents or ionic liquids. The comparison of PEO/LiTFSI based on raw PEO and ultrafiltrated one, shows unambiguously the impact of unentangled oligomers not only on ionic transport but also on mechanical behaviour. Conductivity, cationic transference numbers and storage modulus data go in the same direction and the cationic conductivity (*O/Li=30*) is divided by 2, following PEO purification.

Keywords: PEO, POE, immobile solvent, ionic transport, polymer electrolyte, purification

1. Introduction

Current and future battery growth is driven by the new markets, i.e. electric mobility and renewable electricity storage. The transposition of low capacity Li-ion batteries, long time confined to portable electronics, to high capacity batteries faces, at short to mid-term, three main issues namely, cost-cutting, safety improvement and progressive scarcity in lithium ores. Regarding cost-cutting, it depends not only on the material chemistry (*electrodes & electrolytes*), but also on a neat increase of electrodes thicknesses and, therefore, of their areal capacity, which allows decreasing the surface of separator and current collectors as well as the electrolyte amount [1]. On the other hand, safety can be improved by using All-Solid-State Batteries (ASSB) but, due to solid electrolyte/solid electrodes interfaces issues, ASSB are mainly limited to microbatteries. Lithium polymer batteries, LPB, were validated in 1995 by Gauthier et al. [2] on 10 Wh prototypes (Li/VO_x). Based on solvent-free polyether electrolytes, LPB are currently revisited, owing to their safety asset (very high Flash Point, Fp) and their ability to absorb the volume changes of electrodes. As thick binder-free ceramic electrodes can be reversibly cycled [3], ASSB based on solvent-free polymer electrolyte [4] can be considered, meeting both safety (Fp) and cost-cutting (high areal capacity) requirements. Among the poly(oxyalkylene)-based electrolytes, the host polymer, poly(oxypropylene) POP (*or PPO*) undergoes microphase separation [5], while poly(oxytetramethylene) (*or PTHF*) exhibits conductivities significantly lower than POP and poly(oxyethylene) POE (*or PEO*) [6]. The main limitations of high molecular weight POE homopolymers are well-identified: (i) high crystallinity ratio, leading to poor conductivities at r.t, (ii) poor mechanical strength above the melting point of POE electrolytes and (iii) an anodic stability limited to about 3.9 V *vs* Li/Li^+. Salts based on bulky anions as LiTFSI [7[8] and Li methide were found to decrease crystallinity and melting temperature of POE-electrolytes [9], without producing any improvement regarding the mechanical strength

issue. As polymer electrolytes don't include any macroporous separator, they must sustain, without creeping, 90°C (*operating temperature range of LPB: 60 to 90°C*) and even retain their mechanical integrity up to at least 160°C. POE networks based electrolytes made of copolymers [10[13] and polycondensates [14-[16] allow both, suppressing crystallinity and avoiding creeping at high temperature. Nonetheless, these promising materials are not commercially available. Due to its availability in a wide range of molecular weights, POE is therefore extensively used in the polymer electrolytes literature, being considered as the reference host polymer for solvent-free polymer electrolytes. At salt concentrations compatible with LPB, i.e. $20 \leq O/Li \leq 30$, the amorphous networked electrolytes exhibit much higher conductivities than the POE ones up to their melting. On the other hand, the latter lead generally to conductivity maxima higher than that of cross-linked electrolytes. This gap whether originates from defects-free linear POE leading to a perfect macromolecular solvent, from the stiffening induced by the cross-linking of polyether chains or, possibly, from low molecular weight unentangled chains (molecular weight below the entanglement threshold, i.e. 3,200 g/mole) present in the commercial POE grades. Indeed, Vincent et al. [17], through electrochemical impedance spectroscopy and PFGNMR performed on POE electrolytes, in a wide range of POE molecular weights, demonstrated that below this threshold, Mg^{2+} moves together with the oligoether chains and, beyond, becomes immobile. Suspecting the gap in conductivity maxima might result from the presence, in commercial POE, of unentangled oligomers, we performed ultrafiltration of POE aqueous solutions using a membrane cut-off at 3,000 g/mole. A POE grade of 300,000 g/mole was selected as we previously proved that POE solutions of higher molecular weights undergo dramatic chain breakings, even when a mild stirring as magnetic stirring was applied [18]. This contribution reports on the electrochemical (conductivities and cationic transference

numbers) and thermomechanical discrepancies between, on the one hand POE electrolytes consisting on unpurified commercial POE (raw-POE) and, on the other hand, those consisting on the oligomers-free one (UF-POE).

2. Experimental

2.1. Materials and films processing

POE 300,000 g/mole was dissolved in distillated water (8 wt.%) and ultrafiltrated under pressure through a membrane (cut-off: 3,000 g/mole) using a Millipore 8200. The ultrafiltration cell is equipped with a magnetic stirrer in order to avoid aggregate formation and subsequent pore clogging. Ultrafiltration must be carried out on diluted solution. Typically, purification of a POE sample requires three days of ultrafiltration. After lyophilization, the obtained powder and LiTFSI were dissolved in acetonitrile and cast in a glove-box under argon atmosphere. After a slow removal of acetonitrile, the films were heated under vacuum.

2.2. Dynamic mechanical analysis (DMA)

Dynamic mechanical analysis (DMA) measurements were carried out with a TA instruments DMA Q800 analyzer working in tensile mode. A strain magnitude fixed at 0.05% guarantees that tests were made in the linear viscoelastic domain. Measurements on the thin samples were performed in isochronal condition (1 Hz) in the temperature range from -100 to +100°C at 3°C/min.

2.3. Differential scanning calorimetry (DSC)

Glass transition temperatures, T_g, melting temperatures, T_m, and the enthalpy of fusion, ΔH_m, were measured by DSC (Differential Scanning Calorimetry) using a GC20 from

Mettler Toledo. Samples of approximatively 5 μg were introduced in aluminum pans in a glove box, under argon. In a typical procedure, samples were submitted to two heating cycles from -100 to 100°C with a heating ramp of 10°C/min. During the cooling step (from room temperature to -100°C and from 100 to -100°C), the cooling rate was set at 20°C/min. Before the heating or cooling steps, samples were submitted to an isotherm of 3 minutes in order to stabilize the temperature.

2.4. Conductivity measurements

Conductivity measurements were carried out by electrochemical impedance spectroscopy using a HP4192A impedance analyzer, over the frequency range 5 Hz-13 MHz. The samples were sandwiched, under argon, between two stainless steel electrodes in a Swagelok cell with Teflon o-rings. Measurements were performed in the temperature range from 20°C to 80°C; values were taken in both, heating (from 20 to 80°C, up) and cooling (from 80 to 20°C, down) steps. A dwell time of one hour was set between measurements.

3. Results and discussion

3.1. Differential scanning calorimetry (DSC)

To investigate the impact of ultrafiltration on the characteristic temperatures, as well as the crystallinity content, we performed DSC and TGA characterizations. However, since no significant differences on behavior were noticed regarding thermogravimetric analyses, TGA measurements were discarded from this contribution. Table 1 gathers the thermal characteristics, obtained during the second heating cycle, of raw and ultrafiltrated samples at two O/Li compositions.

At high LiTFSI concentration, i.e. around O/Li = 8, the crystallinity seems to vanish but it is not suppressed in high molecular weight POE electrolytes, where it slowly reappears. The delay in crystallization is however sufficient to allow the conductivities, in an evenly amorphous POE electrolyte, to be significant from ambient temperature on. Furthermore, by quenching melted samples, it is possible to determine the T_g of an amorphous phase unconstrained by the crystalline one. Using lower salt concentrations, i.e. 20 and 30, leads to polymer electrolytes that we could not quench efficiently into their amorphous state. Thus, as usual, the measured T_g of such semi-crystalline electrolytes are not representative of the segmental mobility [19]. Due to both Li^+ interchain solvation, i.e. transient cross-linking, and the non-specific interaction occurring in any mixture, as described by the Flory-Fox semi-empirical relationship [20], a T_g increase with the salt concentration would be expected. On the contrary, it was found that T_g is unmodified or is even slightly increased. Indeed, increasing LiTFSI concentration decreases crystallinity and melting temperature, T_m. Due to the crystallinity decrease, so to the decrease in the constraining of amorphous phase, the T_g measured is artificially lower for O/Li=20 compared to O/Li=30. Nevertheless, the gaps found in crystallinity and T_m for raw and UF-POE based electrolytes are not significant for both salt concentrations.

3.2. Thermomechanical characterization

The thermomechanical behavior of the raw and ultrafiltrated POE host polymers was found to be similar. Therefore, as shown in figure 1, DMA measurements were afterwards extended to their LiTFSI-based polymer electrolytes, prepared with a salt concentration O/Li=30. At low temperatures, between -100 and -40°C, the storage modulus, E', remains constant and close to approximately 4 GPa. Afterwards, E' declines sharply, down to 500 MPa at -20°C. The relaxation α, T_α, measured at the maximum of tan δ, is associated to

the molecular motions of the amorphous phase segments and characterizes the drop in storage modulus associated to the glass transition of the polymer electrolyte.

Although very close, the tan δ maxima for electrolytes based on raw and ultrafiltrated POE were found to be – 28.9º C and – 24.6ºC, respectively. We ascribe this small gap to the plasticizing effect of the unentangled oligomers contained in the raw POE. Both T_α values exceed by 6 to 9ºC the T_g measured by DSC. The T_α-T_g gap is related to the thermal treatment applied to the samples during DSC measurements, which involves heating followed by cooling, while samples do not undergo any thermal treatment before DMA measurements. Such heating-cooling cycle performed during DSC decreases the crystallinity and, consequently, the constraining of the amorphous phase that slows down the chain mobility, *vide supra*. Regarding the electrolyte behavior around T_m and beyond, the electrolyte based on the raw POE exhibits a classical behavior, experiencing creeping above T_m. A distinct and interesting behavior of the ultrafiltrated POE-based electrolyte, which exhibits a plateau around 0.5 MPa after T_m and up to at least 100°C, must be highlighted. This unexpected reinforcement is ascribable to interchain Li^+ solvation (transient cross-links) that, in the case of the ultrafiltrated material, occurs between entangled chains while it probably involves unentangled chains, i.e. oligomer ⇔ oligomer and oligomer ⇔ long POE chain in the case of the raw POE.

3.3. Transport properties

3.3.1. Conductivity comparison

The Arrhenius plots of POE-electrolytes are gathered in Figure 2. Impedance measurements were performed either by heating from 20º C to 80ºC (up) and by cooling from 80º C (down) to 21ºC. The former reveals the material performances in its equilibrated state while the latter, due to crystallization delay (supercooling), artificially

increases the conductivities below T_m. For convenience, the Arrhenius plots were divided into "down" and "up" for cooling and heating, respectively, the data 'up' appearing as insets. Hosting LiTFSI in UF-POE results in a conductivity decrease for the whole temperature range, when compared to LiTFSI hosted by the raw POE. For instance, the conductivity gap at the salt concentration O/Li=20 reaches, at 70°C, 37%. As expected for both electrolytes, based on raw POE and UF-POE, the conductivity was significantly lower for both salt concentrations at temperatures below T_m in the "up" Arrhenius plots. At room temperature, the conductivity gap between UF and raw POE electrolytes exceeds 500% for both salt concentrations and is roughly the same in "up" and "down" impedance measurements. This neat conductivity decrease could be ascribed to the removal of unentangled oligomers, which behave as non-volatile plasticizers. These results are supported by LiTFSI conductivity data collected by Balsara et al. [21] on a wide range of quasi-monodisperse POE solvents.

In figure 3 we compare the conductivity behavior of UF-POE electrolytes with those of optimized POE network ones, moderately cross-linked and amorphous from roughly 25ºC [22]. The latter, which do not creep, are obtained from the cross-linking of a pre-polymer that underwent ultrafiltration (cut-off: 3,000 g/mole) and partial hydrogenation (75%). This comparison unambiguously demonstrates that optimized polymer electrolytes can lead, in a wide temperature range, to significantly improved performances with regard to electrolytes based on UF-POE.

3.3.2. Transference numbers

Beyond ionic conductivity measurements, the cationic transference number is a key parameter, since it highly influences cationic conductivity and conductance. The cationic transference numbers, T^+, were determined by both electrochemical impedance

199 spectroscopy and Pulse Field Gradient NMR (PFGNMR). Even though several T^+ have
200 been previously reported on POE/LiTFSI electrolytes based on raw POE, we opted for its
201 characterization, as (i) the POE applied usually has very high molecular weight,
202 undergoing chain scissions during sample preparation, and (ii) a thorough comparison
203 requires using the same material and protocols. T^+ determinations were performed at 70ºC
204 in order to discard any doubt about a possible creping of POE electrolytes during the EIS
205 experiments.
206
207 **T^+ from PFGNMR experiments**
208 Table 2 collects the data obtained for the concentration O/Li=30. From the obtained data,
209 it can be seen that the Li^+ diffusion coefficient is only slightly increased (~ 4.5%), while
210 the anion diffusion coefficient remains almost unchanged. Indeed, the gap in Li^+ mobility
211 remains in the margin of error. As removed materials (i) are mainly unentangled
212 oligomers and not volatile molecules and (ii) are embedded in the POE long chains, the
213 results are not surprising as, especially, the samples do not undergo electrical polarization.
214
215 **T^+ from EIS experiments**
216 Cationic transference numbers were determined using the Sorensen method [23]. From
217 EIS, it was observed that T^+ increases by ~ 30% when comparing LiTFSI hosted in UF-
218 POE (0.13) and in raw-POE (0.17). From these data, we can infer that unentangled
219 oligomers, which should have the same solvating ability versus Li^+ than the POE long
220 chains, move together with the anion and cation. These results are in line with Shi results
221 [24]. The dual decrease in ionic conductivity and T^+ in UF-POE electrolytes, leads to a
222 substantial decrease in cationic conductivity ($\sigma^+ = \sigma.T^+$), which drops by more than 100%
223 as compared to the unpurified electrolyte (Table 3).

4. Conclusions

Both electrochemical impedance spectroscopy, i.e. ionic conductivities and cationic transference numbers data, as well as Dynamic Mechanical Analyses are in perfect agreement and highlight the significant influence of unentangled oligomers on the ionic transport in LiTFSI/raw POE polymer electrolytes. Polyether networks alternatives to POE undergoing generally, a purification step, e.g. by precipitation, lead to the partial or total removal of unentangled oligoether chains. Hence, their electrolytes should be compared not to raw POE electrolytes but to ultrafiltered ones. In that sense, some of them should exhibit higher conductivities and cationic conductivities, in the whole range of LPB operating temperatures (25 to 90ºC). Pending industrial development of POE alternatives, POE electrolytes remain attractive even though it would be difficult to cut the crystallinity and lower significantly their T_m, at the moderate salt concentrations required in LPB. From a practical point of view, why removing by ultrafiltration unentangled oligomers that increase both conductivity and cationic transference numbers? Indeed ultrafiltration (i) allows both removing oligomers but also impurities and (ii) leads to aqueous POE solutions that can be cast into polymer electrolyte films and can be used to formulate the positive electrode without using organic solvents. Even though polymer electrolytes based on ultrafiltered POE have slightly higher mechanical strength than those based on raw POE, this gain nevertheless remains insufficient both to thinner the electrolyte film, in order to optimize the ionic conductance, and to protect the battery from a thermal runaway. Fortunately, this poor thermomechanical stability it can be remedied by a nanocomposite approach. Thanks to the formation of a network by hydrogen bonding and to the tremendous E' of the highly crystalline nanofibers, crystalline nanocellulose, NCC, hugely increases the storage modulus of POE electrolytes

[25] without compromising the ionic conductivity and allows a sharp thickness of the electrolyte film to be considered. Regarding a possible thermal runaway, as the NCC network starts decomposing from roughly 250ºC, it provides an indisputable safety asset to LPB. It can be pointed out that the ultrafiltered solutions of POE, free of oligomers and impurities, can be blended to the NCC aqueous dispersions to prepare the nanocomposite polymer electrolytes by an overall green approach.

5. Acknowledgments

Jean-Yves Sanchez acknowledges the CONEX Programme, funding received from Universidad Carlos III de Madrid, the European Union's Seventh Framework Programme for research, technological development and demonstration (Grant agreement nº 600371), Spanish Ministry of Economy and Competitiveness (COFUND2013-40258) and Banco Santander. Amadou Thiam acknowledges ANR for his fellowship. Yannick Molméret acknowledges KICINNO Energy for the granting of his post-doc fellowship, in the frame of the project PENLiB coordinated by Prof. Jean-Yves Sanchez.

6. References

[1] M.Singh, J.Kaiser, H.Hahn, Thick Electrodes for High Energy Lithium Ion Batteries, J.Electrochem.Soc. 162(7) (2015) A1196.

[2] M.E. Sotomayor, C. de la Torre-Gamarra, W. Bucheli, J.M. Amarilla, A. Varez, B. Levenfeld, J.Y. Sanchez, Additives-free $Li_4Ti_50_{12}$ thick electrodes for Lithium-ion batteries with high electrochemical performances, J. Mater. Chem. A. 6 (14) (2018) 5952.

[3] J.Y. Sanchez, M.E. Sotomayor, C. de la Torre-Gamarra, C. Martinez-Cisneros, J.M. Amarilla, B. Levenfeld, A. Várez, Thick LTO ceramic electrodes: processing and performances, 16th International Symposium on Polymer Electrolytes (ISPE-16), Yokohama, Japan, June 2016.

[4] M.Gauthier, A.Bélanger, P.Bouchard, B.Kapfer, S.Ricard, G.Vassort, M.Armand, J-Y.Sanchez, L.Krause, Large Lithium Polymer Battery Development: the Immobile Solvent concept, J.Power Sources 54 (1) (1995) 163

[5] C.Vachon, C.Labrèche, A.Vallée, S.Besner, M.Dumont, J.Prudhomme, Microphase separation and conductivity behavior in poly(propylene oxide)-Lithium salt electrolytes, Macromolecules 28(6) (1995) 5585

[6] F.Alloin, J-Y.Sanchez, Electrochemical comparison of several polyethers, Electrochimica acta, 43(10-11) (1998) 1199.

[7] S.Sylla, J-Y.Sanchez, M.Armand, Electrochemical study of Linear and Cross-linked POE-based polymer electrolytes, Electrochimica acta 37(9) (1992) 1699.

[8] A.Vallée, S.Besner, J.Prudhomme, Comparative study of poly(ethylene oxide) electrolytes made with $LiN(CF_3SO_2)_2$, $LiCF_3SO_3$ and $LiClO_4$. Thermal properties and conductivity behavior, Electrochimica acta 37(9) (1992) 1579.

[9] D.Benrabah, D.Baril, J-Y.Sanchez, M.Armand, G.G.Gard, Comparative study of new poly(oxyethylene)-Li salts complexes, J.Chem.Soc. - Faraday Transactions, 89(2) (1993) 355.

[10] F.Alloin, J-Y. Sanchez, New solvating polyether networks, Electrochimica Acta 40 (1995) 2269.

[11] M.Watanabe, A.Nishimoto, Effect of network structures and incorporated salt species on electrochemical properties of polyether-based polymer electrolytes, Solid State Ionics 79 (1995) 306

[12] F. Alloin, J.-Y.Sanchez, Partial hydrogenation of unsaturated polyethers; A convenient route to curable polymers for Lithium Batteries, Journal of Polymer Science: Part A: Polymer Chemistry (38) (2000) 2900.

[13] R.Khurana, J.L. Schaefer, L.A.Archer, G.W.Coates, Suppression of Lithium Dendrite Growth Using Cross-Linked polyethylene/poly(ethylene oxide) Electrolytes: A New Approach for Practical Lithium-Metal Polymer Batteries, J.Am.Chem.Soc. 136 (2014) 7395.

[14] H. Cheradame, J. L. Souquet et J. M. Latour, Ionic conductivity of macromolecular networks I- Polyether filled with Sodium Tetraphenylboride, Mater. Res. Bull 15 (1980) 1173

[15] D.Benrabah, J-Y.Sanchez, M.Armand, New Polyamide-ether electrolytes, Electrochimica acta 37 (9) (1992) 1737.

[16] F.Alloin, J-Y.Sanchez, M.Armand, Electrochemical behavior of lithium electrolytes based on new polyether networks, J.Electrochem.Soc. 141(7) (1994) 1915.

[17] C.A.Vincent, Ion transport in Polymer Electrolytes, Electrochimica Acta 40 (1995) 2035.

[18] F.Bossard, N.El Kissi, A.D'Aprea, F.Alloin, J-Y.Sanchez, A.Dufresne, Influence of dispersion procedures on rheological properties of aqueous solutions of high molecular weight PEO, Rheologica Acta 49(5) (2010) 529

[19] C.S.Martinez-Cisneros, B.Levenfeld, A.Varez, J-Y.Sanchez, Development of sodium-conducting polymer electrolytes: comparison between film casting and films obtained via green processes, Electrochimica acta 192 (2016) 456.

[20] E. Paillard, C. Iojoiu, F. Alloin, J. Guindet, J.-Y. Sanchez, Electrochemical investigation of polymer electrolytes based on lithium 2- (phenylsulfanyl)-1,1-2,2 tetrafluoroethanesulfonate, Electrochimica acta 52 (2007) 3758

[21] A.A.Teran, M.H.Tang, S.A.Mullin, N.P.Balsara, Effect of molecular weight on conductivity of polymer electrolytes, Solid State Ionics 203 (2011) 18.

[22] A.Thiam, C.Iojoiu, J-C.Leprêtre, J-Y.Sanchez, Lithium salts based on a series of new anilinyl-perfluorosulfonamide salts and their polymer electrolytes, *J.Power Sources* 364 (2017) 138.

[23] P. R. Sorensen, T. Jacobsen, Conductivity, charge transfer and transport number- An AC investigation of the polymer electrolyte LiSCN-poly(ethylenexide), *Electrochimica acta* 27(12) (1982) 1671

[24] J. Shi, C. A. Vincent, The effect of molecular weight on cation mobility in polymer electrolytes, *Solid State Ionics* 60(1-3) (1993) 11

[25] Masa.Samir, F.Alloin, J-Y.Sanchez, A.Dufresne, Cellulose Nanocrystals reinforced poly(oxyethylene), Polymer, 45(12) (2004) 4149

339 # Tables

340

341 **Table1.** Thermal characteristics of raw and ultrafiltrated POE/LiTFSI samples

	T_g(°C)	T_m(°C)	ΔH_m(J/g)	X(%)
POE_O/Li20 raw	-34	43	56.4	27.5
POE_O/Li20 UF	-36	43	54.9	26.7
POE_O/Li30 raw	-34	51	83.7	40.8
POE_O/Li30 UF	-34	49	84	40.9

342

343 **Table 2.** Diffusion coefficients obtained for O/Li=20 usingPFGNMR

Sample	Temp. ºC	^{7}Li ($m^2.sec.^{-1}$)	^{19}F ($m^2.sec.^{-1}$)	T^+
UF-POE/LiTFSI-O/Li 30. Nº.1	70	$3.10.10^{-12}$	$1.75.\ 10^{-11}$	0.15
UF-POE/LiTFSI-O/Li 30. Nº.2	70	$3.10.10^{-12}$	$1.80.\ 10^{-11}$	0.147
Raw-POE/LiTFSI-O/Li 30.	70	$3.24.10^{-12}$	$1.76.\ 10^{-11}$	0.155

344

345 **Table 3.** Diffusion coefficients obtained from EIS experiments

O/Li = 30	σ (70°C) $mS.cm^{-1}$	T^+	$\sigma.T^+$
Raw-POE/LiTFSI	0.63*4*	0.17	0.108
UF-POE/LiTFSI	0.36*6*	0.13	0.048

346

347

348 # Figures

349

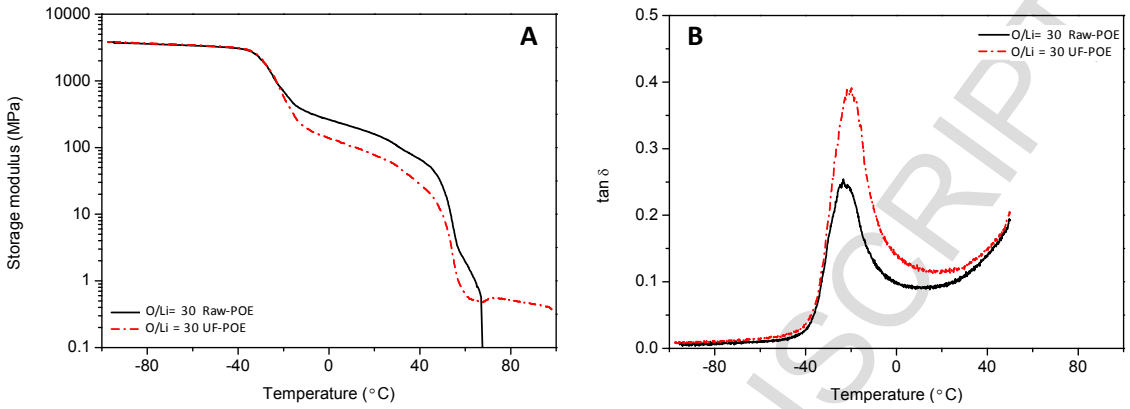

350

351 **Figure 1.** Storage modulus E' (A) and Tan δ (B) *vs* temperature at 1Hz for raw and

352 ultrafiltrated POE at O/Li=30.

353

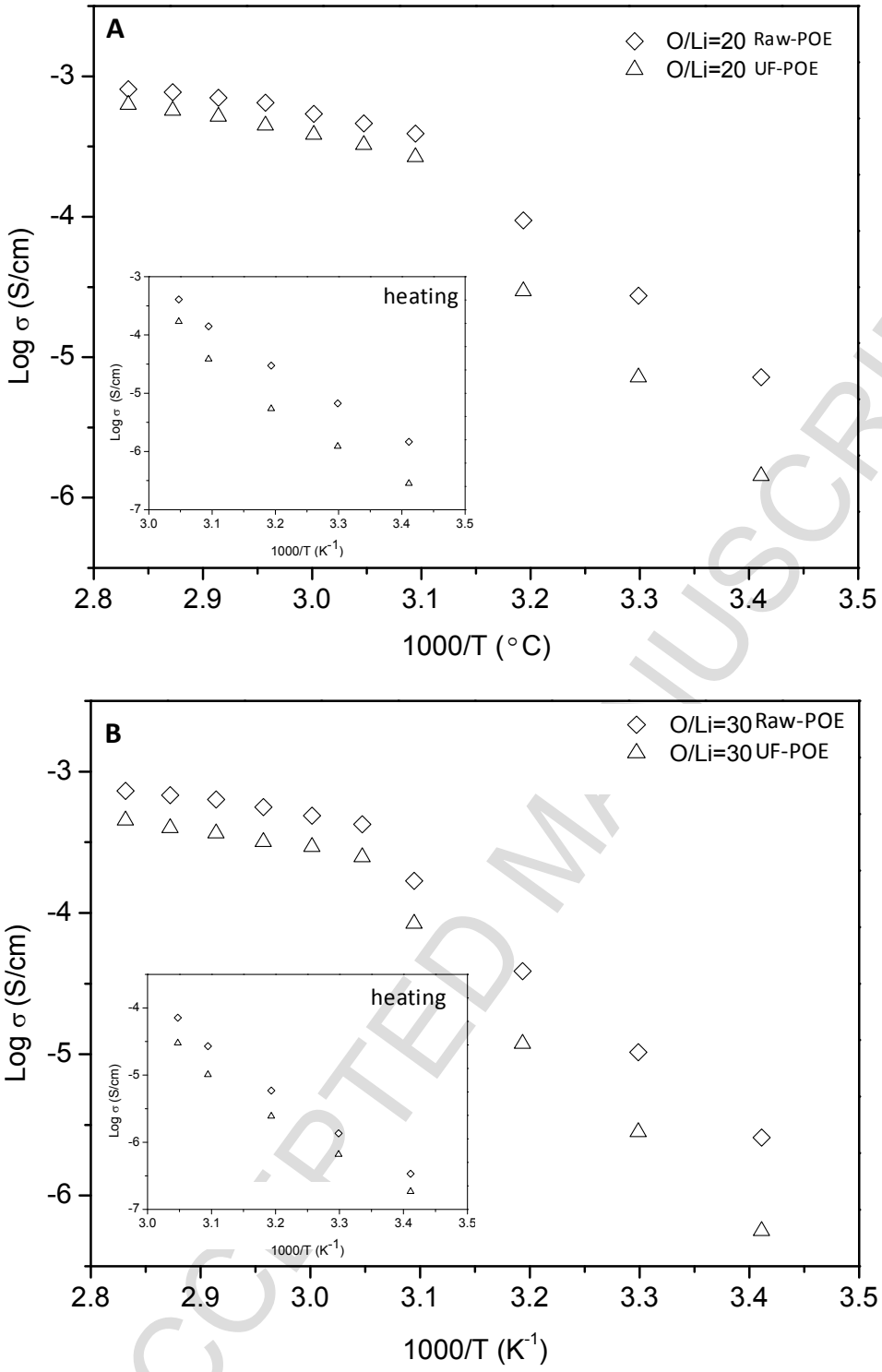

354

355 **Figure 2.** Conductivity measurements at different O/Li ratios: 20 (A) and 30 (B) while
356 cooling and heating (insets) for samples based on raw and ultrafiltrated POE.

357

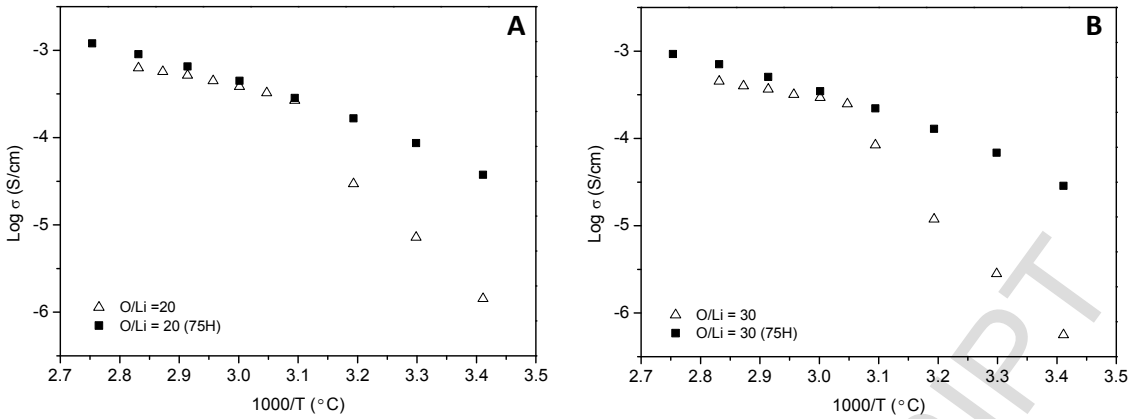

358

359 **Figure 3**. Comparison of conductivity performance of ultrafiltrated and partial

360 hydrogenated polymer electrolytes with a O/Li ratio of 20 (A) and 30 (B).

361

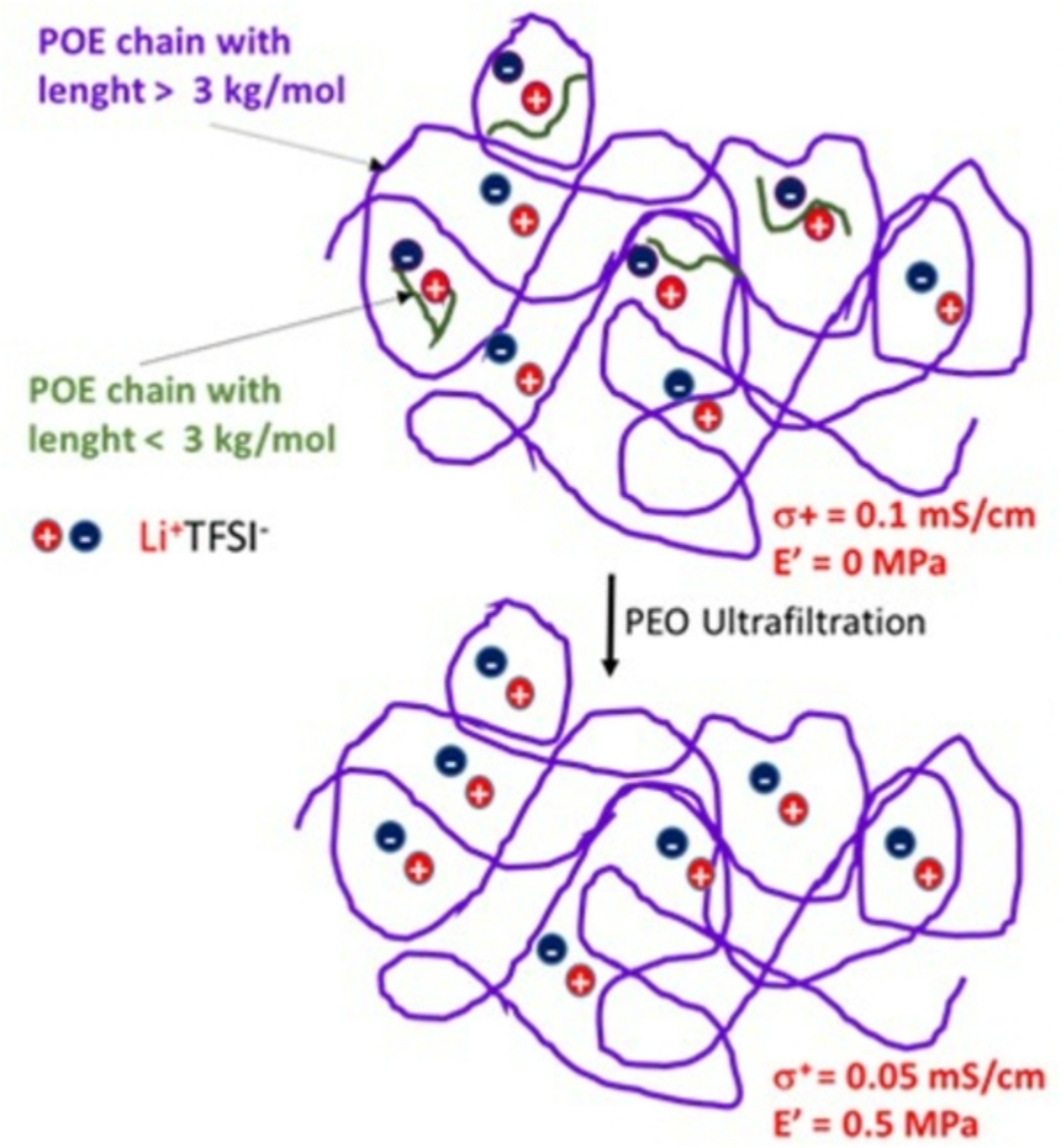
POE chain with
lenght > 3 kg/mol
POE chain with
lenght < 3 kg/mol
Li+TFSI-
σ+ = 0.1 mS/cm
E' = 0 MPa
PEO Ultrafiltration
σ+ = 0.05 mS/cm
E' = 0.5 MPa